Periodic Trends for Transition Metal Dihydrides MH_2, Dihydride Dihydrogen Complexes $MH_2 \cdot H_2$, and Tetrahydrides MH_4 (M = Ti, V, and Cr)

Buyong Ma, Charlene L. Collins, and Henry F. Schaefer III*

Contribution from the Center for Computational Quantum Chemistry, The University of Georgia, Athens, Georgia 30602

Received April 28, 1995[⊗]

Abstract: *Ab initio* quantum mechanical methods were employed to study the periodic trends of transition metal (M = Ti, V, and Cr) hydrides MH_2, dihydride dihydrogen complexes $MH_2 \cdot H_2$, and tetrahydrides MH_4. The configuration interaction with single and double excitations (CISD), coupled cluster including all single and double substitutions (CCSD) methods, and CCSD with the effects of connected triple excitation added perturbatively [CCSD(T)] were used with the TZP, TZP+f, and TZP(f,d) basis sets. The ground electronic states for TiH_2 and VH_2 were found to be $^3B_1$ and $^4B_2$, respectively. The bond angles for the TiH_2 and VH_2 molecules are predicted to be 142° and 139°, respectively, at the TZP(f,d) CISD level of theory. On the low-spin potential energy surfaces, the lowest lying electronic states for the TiH_2, VH_2, and CrH_2 molecules are $^1A_1$, $^2A_1$, and $^3B_2$, respectively. The energy separations between the ground state and the lowest lying low-spin state were found to be 33, 40, and 59 kcal mol^{-1} for the TiH_2, VH_2, and CrH_2 molecules, respectively, at the TZP CCSD level of theory. The binding energies of the dihydride dihydrogen complexes decrease with increasing atomic number. The d $\rightarrow \sigma^*$ back donation dominates the periodic trend for the formation of low-spin $MH_2 \cdot H_2$ complexes. All three $MH_2 \cdot H_2$ complexes are in the high-spin ground state, primarily due to the fact that the corresponding parent dihydrides have high-spin ground states. The low-spin dihydrides interact with the H_2 moiety more strongly than do the high-spin species. The d $\rightarrow \sigma^*$ back donation was so strong for the low-spin TiH_2 that H_2 dissociates without barrier upon contact with singlet TiH_2 to form TiH_4. Due to the Jahn−Teller distortion the ground state of VH_4 is the $^2A_1$ electronic state having D_{2d} symmetry. TiH_4 is predicted to lie 9 kcal mol^{-1} lower in energy than its ground state $MH_2 \cdot H_2$ isomer, whereas VH_4 and CrH_4 are higher in energy by 22 and 39 kcal mol^{-1}, respectively, at the TZP CCSD level of theory. However, comparing MH_4 and $MH_2 \cdot H_2$ in the same spin state, MH_4 is always lower in energy than its dihydrogen complex isomer, $MH_2 \cdot H_2$, on the low-spin potential energy surface. Comparison between the present work and experimental IR spectra from the matrix isolation of the cocondesation of transition metal atoms (Ti, V, and Cr) with H_2 molecules confirmed the existence of $CrH_2 \cdot H_2$ by identifying a strong unique absorption at 1510 cm^{-1}. It was found $TiH_2 \cdot H_2$ rather than TiH_2 may be observed experimentally, and that $VH_2 \cdot H_2$ may be formed concomitantly with the VH_2 molecule.

1. Introduction

Transition metal hydrides have long been of interest because of their key role in catalytic hydrogenation processes.[1−8] The recent recognition of the so-called nonclassical hydride complexes, containing the dihydrogen ligand, has opened a new field of investigation.[1−3] The discovery[1] of the first dihydrogen complex by Kubas et al. was one of the most exciting results in inorganic chemistry in the 1980s. For the new dihydrogen complexes, the H_2 ligand was shown to be bound as an intact molecule (structure **A**) rather than in the usual dihydride form (**B**).

The bonding in metal dihydrogen complexes (**A**) has been described using a model similar to that for the binding to ethylene and other related ligands.[2] There are two important factors in such a model. One is that the electron donation from the filled H_2 (σ) orbital to the empty M (d_σ) orbital weakens, but does not break, the H−H bond because the resulting two-electron, three-center orbitals are delocalized over all three atoms. Another is the "back-donation" of electrons from the filled metal d_π orbitals into the empty H_2 (σ^*) orbital, which tends to break the H−H bond.

Although the initial focus of work in the field has been the synthesis of new dihydrogen complexes as well as the description of their structure and bonding, more recent work has addressed reactivity of these interesting molecules, including dihydrogen/dihydride interconversion.[2c] There is a set of obvious questions,[2a] including: what factors influence the

[⊗] Abstract published in *Advance ACS Abstracts,* January 15, 1996.

(1) (a) Kubas, G. J.; Ryan, R. R.; Swanson, B. I.; Vergamini, P. J.; Wasserman, H. J. *J. Am. Chem. Soc.* **1984**, *106*, 451. (b) Kubas, G. J. *Acc. Chem. Res.* **1988**, *21*, 120; *Comments Inorg. Chem.* **1988**, *7*, 17.

(2) (a) Burdett, J. K.; Eisenstein, O.; Jackson, S. A. In *Transition Metal Hydrides*; Dedieu, A., Ed.; VCH Publisher, Inc.: New York, 1992; p 149. (b) Crabtree, R. H. *Acc. Chem. Res.* **1990**, *23*, 95. (c) Heinekey, D. M.; Oldham, W. J. *Chem. Rev.* **1993**, *93*, 913.

(3) Crabtree, R. H. *Chem. Rev.* **1985**, *85*, 245.

(4) (a) Xiao, Z. L.; Hauge, R. H.; Margrave, J. L. *J. Phys. Chem.* **1991**, *95*, 2696; *J. Phys. Chem.* **1992**, *96*, 636. (b) Van Zee, R. J.; Li, S.; Weltner, W. *J. Chem. Phys.* **1995**, *102*, 4367.

(5) Hood, D. M.; Pitzer, R. M.; Schaefer, H. F. *J. Chem. Phys.* **1979**, *71*, 705.

(6) Thomas, J. R.; Quelch, G. E.; Seidl, E. T.; Schaefer, H. F. *J. Chem. Phys.* **1992**, *96*, 6857.

(7) Demuynck, J.; Schaefer, H. F. *J. Chem. Phys.* **1980**, *72*, 311.

(8) Tyrrell, J.; Youakim, A. *J. Phys. Chem.* **1981**, *85*, 3614.

0002-7863/96/1518-0870$12.00/0

stability of dihydrogen complexes? and, what are the electronic features that stabilize this nonclassic arrangement (**A**) relative to its classical analog (**B**)? Apparently, much more work is required for a complete description of this novel bond and its reactions. Principles that emerge are likely to be relevant to other problems, such as the functionalization of inactivated C−H bonds.[3]

We present here our theoretical study of three of the simplest possible dihydrogen complexes, namely $TiH_2{\cdot}H_2$, $VH_2{\cdot}H_2$, and $CrH_2{\cdot}H_2$. The results include the structures, potential energy surfaces, and vibrational frequencies of related species. For these three complexes, only $CrH_2{\cdot}H_2$ has been observed experimentally, as an intermediate in a matrix isolation IR experiment.[4] The possible existence of $TiH_2{\cdot}H_2$ or $VH_2{\cdot}H_2$ is important since no dihydrogen complex involving Ti or V elements had been reported[2c] as of early 1995. If confirmed to exist, then $TiH_2{\cdot}H_2$, $VH_2{\cdot}H_2$, and $CrH_2{\cdot}H_2$ will be the first homoleptic dihydrogen complex ever reported and would provide important information about dihydrogen complexes, due to the simplicity of the $MH_2{\cdot}H_2$ complexes. Additionally, energetic comparisons with their MH_4 isomers could be used to understand the dihydrogen/hydride interconversion. However, little is known from experiment about MH_4 molecules,[5] even though mono- and ihydrides (MH and MH_2) have been studied intensively. In fact TiH_4, MoH_4, and NbH_4 are the only three tetrahydrides for which there are any significant laboratory data.[4]

Several experiments have been performed to study the cocondensation of light transition metal atoms (Ti, V, and Cr) with hydrogen molecules via matrix isolation, followed by photolysis.[4] Upon analyzing the IR spectra of the photolysis products, Xiao, Hauge, and Margrave assigned the IR frequencies for TiH_2, TiH_4, VH_2, CrH_2, CrH_3, and $CrH_2{\cdot}H_2$ and found all the MH_2 molecules to be bent.[4a] However, the latest ESR studies of VH_2 indicated that VH_2 may be linear, and attempts to observe VH_4 via ESR were not successful, presumably because it could not be prepared in high enough concentrations.[4b] Three questions may arise from these experimental results: 1. Both bent and linear structures[7,8] of TiH_2 and only linear structures[8] of VH_2 have been previously predicted by the Hartree−Fock SCF method. Thus, what are the ground electronic states and structures for the MH_2 molecules at correlated levels of theory? 2. Why was the $CrH_2{\cdot}H_2$ complex detected whereas the $TiH_2{\cdot}H_2$ and $VH_2{\cdot}H_2$ complexes remain elusive? 3. Why was the TiH_4 molecule detected while the VH_4 and CrH_4 molecules remain elusive? Since the main experimental tool employed is analysis of IR spectra and ESR spectra, a detailed study of the potential energy surfaces of MH_2, $MH_2{\cdot}H_2$, and MH_4 molecules is desired.

2. Theoretical Methods

The basis sets used here are the Wachters bases[9] (14s11p6d/10s8p3d) with the addition of two sets of p functions and one set of diffuse d functions for Ti, V, and Cr atoms, respectively. The contraction of the primitive Gaussian bases for the transition metal atoms followed the recommendations of Hood, Pitzer, and Schaefer.[5] Moreover, f type functions are also added into the basis sets for the transition metal atoms. The exponent of the f functions for the Cr atom is taken from ref 10, and those for the Ti and V atoms are obtained by keeping the same α_d/α_f ratio as that for the Cr atom. The exponents for the additional p, d, and f functions are

$$\alpha_p(\mathrm{Ti}) = 0.156 \text{ and } 0.0611;\ \alpha_d(\mathrm{Ti}) = 0.072;\ \alpha_f(\mathrm{Ti}) = 0.9$$

$$\alpha_p(\mathrm{V}) = 0.175 \text{ and } 0.068;\ \alpha_d(\mathrm{V}) = 0.082;\ \alpha_f(\mathrm{V}) = 1.0$$

$$\alpha_p(\mathrm{Cr}) = 0.192 \text{ and } 0.075;\ \alpha_d(\mathrm{Cr}) = 0.0912;\ \alpha_f(\mathrm{Cr}) = 1.14$$

The hydrogen atoms were described using a (5s1p/3s1p) basis set.[11] For the hydrogen atoms in the Cr system, the standard TZP basis set[11] is used. For the hydrogen atoms in the Ti and V systems, the s functions were scaled by a factor of 1.2. Therefore, throughout the text, the TZP basis set refers to Wachters basis (14s11p6d/10s8p3d) for transition metal atoms and the (5s1p/3s1p) basis set for hydrogen atoms; the TZP+f basis set refers to adding f functions to the TZP basis set, and TZP(f,d) refers to adding hydrogen d functions to the TZP+f basis set. Spherical d and f functions were used throughout the text unless Cartesian d and f functions are indicated explicitly.

The simple Hartree−Fock self-consistent-field (SCF) method is found to be insufficient for the system studied here, especially for the dihydrogen complexes—the potential energy surfaces are too different from those reliably determined using correlated levels of theory. Therefore, the configuration interaction method including all single and double excitations (CISD)[12] was used to optimize the geometries, and harmonic vibrational frequencies are evaluated at the CISD level. Finally, single-point energies were obtained with the coupled cluster method with the single- and double-substitutions (CCSD)[13] method, as well as CCSD with the effects of connected triple excitations added perturbatively [CCSD(T)], to recover a larger fraction of the correlation energy and to avoid the size-consistency problem in the CISD method. For the CISD, CCSD, and CCSD(T) methods, the core-like (1s, 2s, and 2p for transition metals) SCF molecular orbitals were constrained to be fully occupied in all configurations. However, no corresponding core-like virtual orbitals were excluded from the CISD, CCSD, and CCSD(T) procedures.

For the linear MH_2 (M = Ti, V, Cr) molecule, the electron configuration for the first 22 electrons is [core] $4\sigma_g^2 3\sigma_u^2$ and the available low-lying molecular orbitals (MO) for the unpaired electrons are likely[7,8] to be $1\delta_g$, $1\pi_g$, and $5\sigma_g$. In C_{2v} symmetry MO labels, the electron configuration for the first 22 electrons is [core] $6a_1^2 3b_2^2$ and the available low-lying molecular orbitals for the unpaired electrons are $7a_1$ and $3b_1$ ($1\delta_g$), $1a_2$ and $4b_2$ ($1\pi_g$), and $8a_1$ ($5\sigma_g$). The computations were performed using the program PSI developed by our research group.[14]

3. Results

A. Electronic Configuration and Equilibrium Geometry of VH_4. The electron configuration for the ground state of TiH_4 is unambiguous: $1a_1^2 2a_1^2 1t_2^6 3a_1^2 2t_2^6 4a_1^2 3t_2^6$. However, for VH_4 there are two possible ground-state electronic configurations in T_d symmetry: $...4a_1^2 3t_2^6 1e$ and $...4a_1^2 3t_2^6 4t_2$, leading to ^2E and $^2T_2$ electron states, respectively. A previous theoretical study[5] of VH_4 predicted that the ^2E state is 36 kcal mol^{-1} lower in energy than the $^2T_2$ state, consistent with classical d orbital splitting by tetrahedral environments. This result was reproduced by the present study. However, because the degenerate 1e molecular orbital (MO) is singly occupied in the ^2E state, a Jahn−Teller distortion is inevitable. As expected, a D_{2d} symmetry structure was found to be 3 kcal mol^{-1} lower in energy than the ideal tetrahedral structure at the TZP SCF level. No further distortion from the D_{2d} structure was found, since

(9) Wachters, A. J. H. *J. Chem. Phys.* **1970**, *52*, 1033.
(10) Scuseria, G. E.; Schaefer, H. F. *Chem. Phys. Lett.* **1990**, *174*, 501.
(11) (a) Huzinaga, S. *J. Chem. Phys.* **1965**, *42*, 1293. (b) Dunning, T. H. *J. Chem. Phys.* **1970**, *53*, 2823. (c) Dunning, T. H.; Hay, P. J. In *Modern Theoretical Chemistry*; Schaefer, H. F., Ed. Plenum Press: New York, 1977; Vol. 3, p 1.
(12) (a) Brooks, B. R.; Laidig, W. D.; Saxe, P.; Goddard, J. D.; Yamaguchi, Y.; Schaefer, H. F. *J. Chem. Phys.* **1980**, *72*, 4652. (b) Rice, J. E.; Amos, R. D.; Handy, N. C.; Lee, T. J.; Schaefer, H. F. *J. Chem. Phys.* **1986**, *85*, 963.
(13) (a) Purvis, G. D.; Bartlett, R. J. *J. Chem. Phys.* **1982**, *76*, 1910. (b) Scuseria, G. E.; Janssen, C. L.; Schaefer, H. F. *J. Chem. Phys.* **1989**, *89*, 7382.
(14) PSI 2. 0.8; Janssen, C. L.; Seidl, E. T.; Hamilton, T. P.; Yamaguchi, Y.; Remington, R. B.; Xie, Y.; Vacek, G.; Sherrill, C. D.; Crawford, T. D.; Fermann, J. T.; Allen, W. D.; Brooks, B. R.; Fitzgerald, G. B.; Fox, D. J.; Gaw, J. F.; Handy, N. C.; Laidig, W. D.; Lee, T. J.; Pitzer, R. M.; Rice, J. E.; Saxe, P.; Scheiner, A. C.; Schaefer, H. F. PSITECH, Inc., Watkinsville, GA, 30677, 1994.

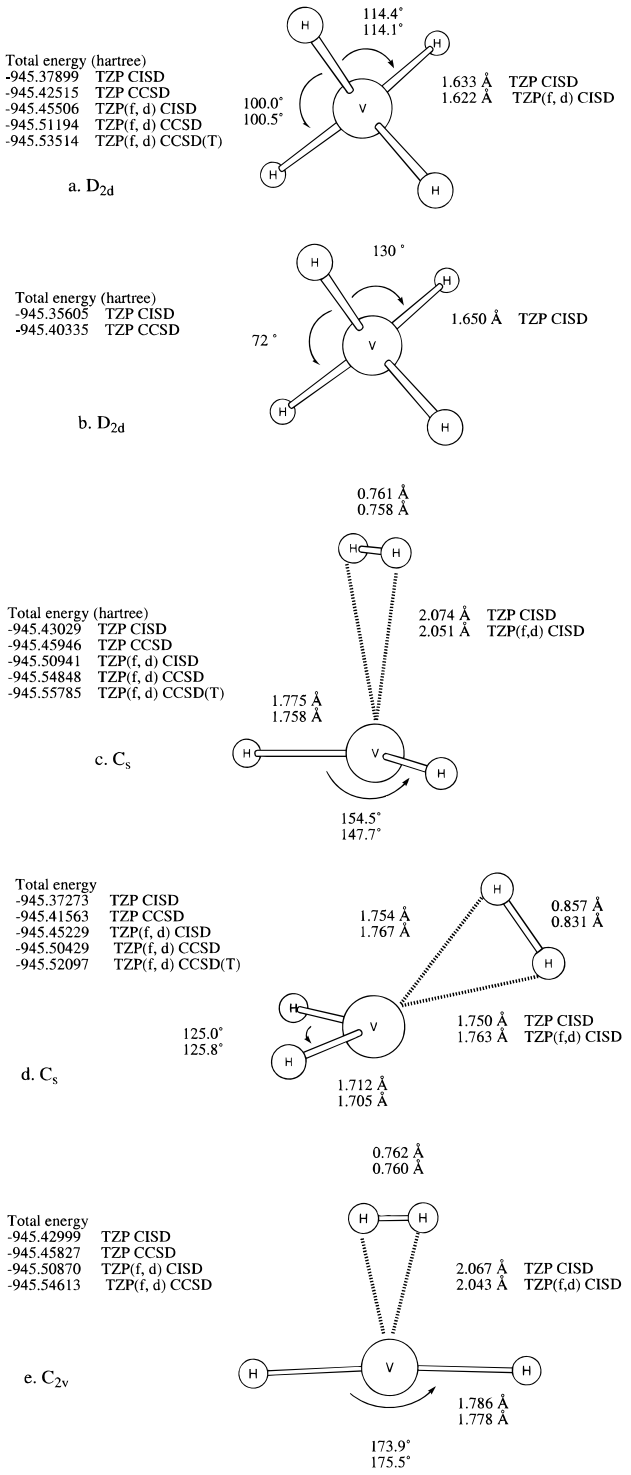

Figure 1. (a) The equilibrium structure and total energy of the $^2A_1$ ground state of the VH_4 molecule. (b) The structure and total energy of the $^2B_1$ state of the VH_4 molecule. (c) The equilibrium structure and total energy of the $^4A''$ state of the $VH_2{\cdot}H_2$ molecule. (d) The structure and total energy of the $^2A''$ state of the $VH_2{\cdot}H_2$ molecule (lowest lying structure on the lowest doublet ($S = {}^1/_2$) potential surface). (e) The structure and total energy of the $^4A_2$ state of the $VH_2{\cdot}H_2$ molecule (local minimum).

the singly occupied MO is totally symmetric in the D_{2d} point group. Therefore, the ground state electron configuration is $1a_1^2 2a_1^2 1b_1^2 1e^4 3a_1^2 2b_1^2 2e^4 4a_1^2 3b_1^2 3e^4 5a_1$, leading to $^2A_1$ symmetry. The bond length for the global minimum structure is 1.622 Å and the bond angles have been distorted from the ideal 109.7° for the tetrahedral structure to 114.1° and 100.5° for the distorted structure at the TZP(f,d) CISD level of theory (Figure 1a). The vibrational frequencies of VH_4 (VD_4) are reported in the supporting information, Table 1. There is another D_{2d}

Table 1. Structures and Energies for the TiH_2 Molecule at the TZP CISD Level of Theory[a]

electronic state	electronic config	rel energy (kcal mol^{-1}) CISD	CCSD[b]	geometry r (Å)	θ (deg)
$^3B_1$	$6a_1^2 3b_2^2 7a_1 3b_1$	0.00	0.00	1.804	148.4
				(1.800)	(143.2)
				1.790	**142.1**
$^3A_1$	$6a_1^2 3b_2^2 7a_1 8a_1$	0.04	0.01	1.805	149.5
		(0.07)	(0.13)	(1.802)	(144.6)
$^3\Delta_g$	$4\sigma_g^2 3\sigma_u^2 1\delta_g 5\sigma_g$	0.64	1.31	1.826	180
$^3A_2$	$6a_1^2 3b_2^2 7a_1 1a_2$	5.61	7.05	1.844	150.8
	$4\sigma_g^2 3\sigma_u^2 1\delta_g \pi_g$	5.97	7.76	1.858	1.80
	$4\sigma_g^2 3\sigma_u^2 1\delta_g^2$	34.56	32.6	1.859	180

[a] The values in parentheses are at the TZP+f CISD level of theory; and the values in boldface are at the TZP(f,d) CISD level of theory. Spherical d and f functions are used. [b] Based on the CCSD single-point energies at the CISD optimized geometries.

Table 2. Structures and Energies for the VH_2 Molecule at the TZP CISD Level of Theory[a]

electronic state	electronic config	rel energy (kcal mol^{-1}) CISD	CCSD[b]	geometry r (Å)	θ (deg)
$^4B_2$	$6a_1^2 3b_2^2 7a_1 3b_1 1a_2$	0.00	0.00	1.766	144.7
				(1.759)	(140.0)
				1.749	**138.8**
$^4B_1$	$6a_1^2 3b_2^2 7a_1 8a_1 3b_1$	2.00	0.66	1.766	144.5
		2.80	**1.50**	**1.749**	**137.4**
$^4A_2$	$6a_1^2 3b_2^2 7a_1 3b_1 4b_2$		0.66	1.766	144.5
$4\Pi_g$	$4\sigma_g^2 3\sigma_u^2 1\delta_g^2 1\pi_g$	0.74	1.79	1.792	180
		1.27	**2.84**	**1.783**	**180**
$^4\Sigma_g^-$	$4\sigma_g^2 3\sigma_u^2 1\delta_g^2 5\sigma_g$	2.80	2.40	1.792	180
$^4A_2$	$6a_1^2 3b_2^2 7a_1 8a_1 1a_2$	5.89	3.45	1.724	131.5
$^4\Delta_g$	$4\sigma_g^2 3\sigma_u^2 1\delta_g 1\pi_g^2$	2.15	4.05	1.791	180
$^2A_1$	$6a_1^2 3b_2^2 3b_1^2 7a_1$	43.02	39.90	1.752	142.5
$^2\Gamma_g^-$	$4\sigma_g^2 3\sigma_u^2 1\delta_g^2 5\sigma_g$	43.99	41.89	1.781	180
$^2A_2$	$6a_1^2 3b_2^2 3b_1^2 1a_2$	47.2	44.06	1.765	145.8
	$4\sigma_g^2 3\sigma_u^2 1\delta_g^2 1\pi_g$	47.79	45.3	1.788	180
$^2B_1$	$6a_1^2 3b_2^2 3b_1^2 4b_1$	133.59		1.631	115.2

[a] The values in parentheses are at the TZP+f CISD level of theory; and the values in boldface are at the TZP(f,d) CISD level of theory. [b] Based on the TZP CCSD single-point energies at the CISD optimized geometries.

structure of VH_4 with electron configuration $1a_1^2 2a_1^2 1b_1^2 1e^4 3a_1^2 2b_1^2 2e^4 4a_1^2 3b_1^2 3e^4 4b_1$, leading to $^2B_1$ symmetry (Figure 1b). This $^2B_1$ state of VH_4 is 13.7 kcal/mol higher in energy than the $^2A_1$ ground state at the TZP CCSD level.

We also studied possible planar configurations of VH_4. For the D_{4h} symmetry conformation, the V−H bond lengths are as long as 1.942 Å, and the energy is very high relative to the ground state. The optimization under planar C_{2v} and C_s symmetry constraints leads to the dissociation of the $VH_2{\cdot}H_2$ complex at both SCF and CISD levels of theory. Therefore, we conclude that it is implausible for the VH_4 molecule to adapt a planar conformation.

B. Equilibrium Geometries and Potential Energy Surfaces of TiH_2, VH_2, and CrH_2. For TiH_2 (d^2), VH_2 (d^3) and CrH_2 (d^4), a major problem is to predict the electronic configuration of the ground state. Demuynck and Schaefer,[7] for example, listed at least ten most plausible electronic states assuming a triplet ground state and C_{2v} symmetry for the TiH_2 molecule. In the present study, we extensively examined the possible low-lying electronic configurations for TiH_2 and VH_2 at the TZP CISD level of theory. The most important results are reported in Tables 2 and 3. The detailed results for CrH_2 will be published separately.[15] With the SCF method, only linear structures were obtained. However, we located both linear

(15) DeLeeuw, B. J.; Schaefer, H. F. *Mol. Phys.* **1995**, *84*, 1109.

Table 3. Structures and Energies for the CrH_2 Molecule at the TZP CISD Level of Theory[a]

electronic state	electronic config	rel energy (kcal mol^{-1})[b] CISD	CCSD	geometry r (Å)	θ (deg)
$^5B_2$	$6a_1^2 3b_2^2 7a_1 3b_1 1a_2 8a_1$	0.00	0.00	1.682	125.2
				1.664	**121.8**
$^5\Sigma_g^+$	$4\sigma_g^2 3\sigma_u^2 1\delta_g^2 1\pi_g^2$	−3.78	1.37	1.736	180
	$4\sigma_g^2 3\sigma_u^2 1\delta_g^2 1\pi_g 5\sigma_g$	56.1	58.6	1.728	180
$^3A_2$	$6a_1^2 3b_2^2 3b_1^2 7a_1 1a_2$	58.2	60.43	1.685	129.5

[a] The values in boldface are at the TZP(f,d) CISD level of theory. [b] The CCSD energies are single-point energies at the CISD optimized geometries.

and bent structures with the CISD method for TiH_2 and VH_2, indicating the importance of including electron correlation effects to investigate these hydrides in a reliable manner. The failure of the SCF level might find its origin in the poor description of the energetics of the atomic states involved in the bent structures compared with those involved in the linear structures.

For the TiH_2 molecule, there are two lowest-lying states which are almost energetically degenerate, having electron configurations of $6a_1^2 3b_2^2 7a_1 8a_1$ and $6a_1^2 3b_2^2 7a_1 3b_1$ in C_{2v} symmetry, leading to $^3A_1$ and $^3B_1$ states, respectively. Both states have bent structures with very similar geometries (Table 1). The $^3A_1$ state was traditionally thought to be the best candidate for the ground state of the TiH_2 molecule.[7,8] However, the $^3B_1$ state is 0.008 kcal mol^{-1} lower in energy at the TZP CCSD level of theory and 0.13 kcal mol^{-1} lower in energy at the TZP+f CCSD level of theory than the $^3A_1$ state. Therefore, the $^3B_1$ state may be the ground state of the TiH_2 molecule, the conclusion also reached recently by Kudo and Gordon.[17] The slightly smaller bond angle for the $^3B_1$ state indicates that the $3d_M-1s_H$ interaction is stronger for the $^3B_1$ state than for the $^3A_1$ state.

The bond angle of TiH_2 is found to be sensitive to the inclusion of f functions. A similar situation was found for the VH_2 molecule (see the following results) and the CrH_2 molecule. The bond angle of TiH_2 is 5° smaller at the TZP+f CISD than that at the TZP CISD level of theory. However, the TiH_2 bond angle is only 1° smaller at the TZP(f,d) CISD than that at the TZP+f CISD level of theory, indicating a trend toward convergence. The TiH_2 bond angle may decrease slightly when a higher level of theory is employed. Therefore, the most reliable TiH_2 bond angle is 142.1°, which is just inside the lower limit of experimental deduction[4a] (147 ± 5°). On the low-spin potential energy surface ([6 0 3 3] closed shell), TiH_2 has a linear structure and is 33 kcal mol^{-1} higher in energy at the TZP CISD level of theory than the global minimum structure (bent $^3B_1$, Table 1).

For the VH_2 molecule, the ground state is unambiguous according to our study. The $^4B_2$ state with electronic configuration $6a_1^2 3b_2^2 7a_1 3b_1 1a_2$ is lowest in energy at both the TZP CISD and TZP CCSD levels of theory (Table 2). Two other states, namely $^4B_1$ and $^4A_2$, with electronic configuations of $6a_1^2 3b_2^2 7a_1 3b_1 8a_1$ and $6a_1^2 3b_2^2 7a_1 3b_1 4b_2$, respectively, are only 0.7 kcal mol^{-1} higher in energy than the $4B_2$ ground state. Tyrrell and Kouakin[8] studied the VH_2 molecule using an *ab initio* ECP method, and obtained a linear structure with electronic configuration $4\sigma_g^2 3\sigma_u^2 1\delta_g 1\pi_g^2$, leading to a $^4\Delta_g$ state. However, we found that the $^4\Delta_g$ state is 4.1 kcal mol^{-1} higher in energy than the $^4B_2$ state at the TZP CCSD level of theory.

There are two conflicting experimental geometries for VH_2. In 1991 Xiao, Hauge, and Margrave[4a] observed the vibrational frequencies for both the symmetric and asymmetric VH_2 stretches, the infrared appearance of which may indicate a bent molecule. However, the 1995 ESR experiments by Van Zee, Li, and Weltner[4b] indicated that the VH_2 molecule is either linear or a bent molecule that is rotating rapidly. Van Zee, Li, and Weltner concluded that the VH_2 is linear since rotation in the different experimental matrices (deuterium, argon, and krypton) seems unlikely. Van Zee concludes that the electronic ground state of VH_2 is of $^4\Sigma_g^-$ symmetry, arising from electron configuration $4\sigma_g^2 3\sigma_u^2 1\delta_g^2 5\sigma_g$. However, our theoretical predictions support the experimental conclusions of Xiao, Hauge, and Margrave, who suggested a bent VH_2 molecule. We predict that the $^4\Sigma_g^-$ state of VH_2 lies 2.40 kcal mol^{-1} above the $^4B_2$ state at the TZP CCSD level (Table 2). It is possible that VD_2 may be nearly linear in a deuterium matrix due to environmental effects (see section C).

The VH_2 bond angle is also sensitive to basis set. This angle is 4.7° smaller at the TZP+f CISD than at the TZP CISD level of theory. The VH_2 bond angle shrinks only 1.2° from the TZP+f CISD to the TZP(f,d) CISD level of theory, indicating a fair convergence. The VH_2 bond angle at the TZP(f,d) CISD level of theory is 138.8°, and that at a higher level of theory might be within the upper limit of the experimentally deduced value[4] (131 ± 5°). On the low-spin potential energy surface, VH_2 also has a bent structure ($^2A_1$, θ = 142.5°, see Table 3)

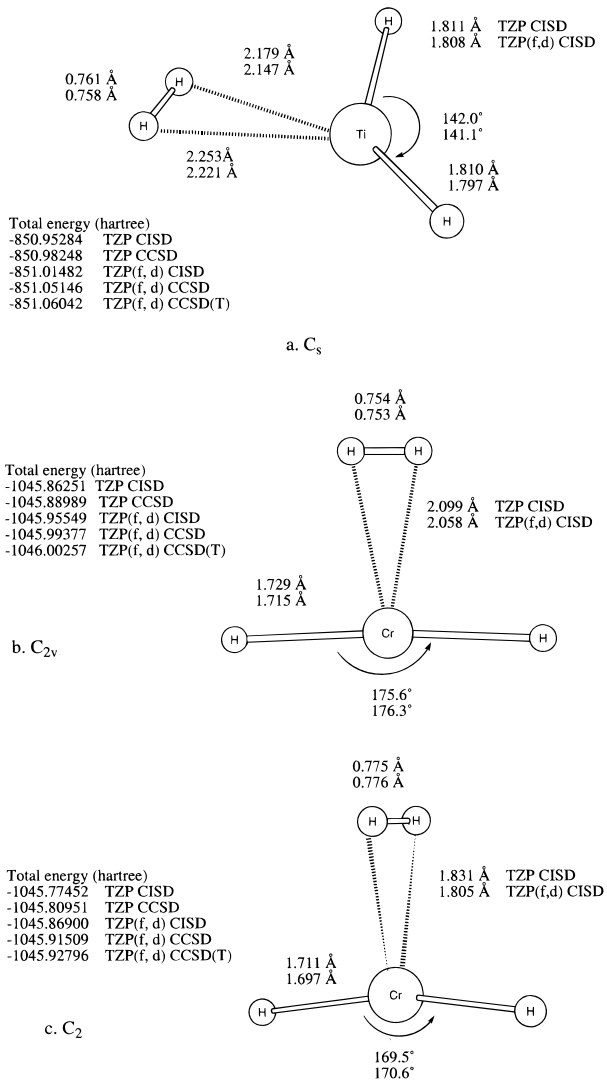

Figure 2. (a) The equilibrium structure and total energy of the $^3A''$ ground state of the $TiH_2{\cdot}H_2$ complex. (b) The equilibrium structure and total energy of the $^5A_1$ ground state of the $CrH_2{\cdot}H_2$ complex. (c) The structure and total energy of the $^3B_2$ state of the $CrH_2{\cdot}H_2$ complex (lowest lying structure on the low-spin potential energy surfaces).

(16) Elkind, J. L.; Armentrout, P. B. *J. Phys. Chem.* **1987**, *91*, 2037.
(17) Kudo, T.; Grodon, M. S. Private communication.

and lies 40 kcal mol^{-1} higher in energy than the global minimum structure ($^4B_2$).

These high-level theoretical results agree with recent experiments[4] in that both TiH_2 and VH_2 are bent. However, the comparison between our theoretical results and the experimental vibrational spectra indicates that the experimental assignments should perhaps be reassessed. We will compare theoretical and experimental assignments later (see Discussion).

We also studied the potential energy surface of the CrH_2 molecule (Table 3). A high-spin $^5B_2$ state bent structure was found to be the equilibrium structure and the detailed results will be published separately.[15] The linear $^5\Sigma_g^+$ ($4\sigma_g^2 3\sigma_u^2 1\delta_g^2 1\pi_g^2$) state of CrH_2 was higher in energy than the ground state CrH_2 by 1.37 kcal mol^{-1} at the TZP CCSD level of theory, and by 4.2 kcal mol^{-1} at the TZ2P+2f CCSD(T) level of theory.[15] On the low-spin potential energy surfaces for CrH_2, there are two low-lying electronic configurations close in energy, namely $4\sigma_g^2 3\sigma_u^2 1\delta_g^2 1\pi_g 5\sigma_g$ and $6a_1^2 3b_2^2 3b_1^2 7a_1 1a_2$ (Table 3). A linear structure ($4\sigma_g^2 3\sigma_u^2 1\delta_g^2 1\pi_g 5\sigma_g$) was found to be lowest in energy on the low-spin potential energy surface but lies 59 kcal mol^{-1} higher in energy than the high-spin quintet state at the TZP CCSD level of theory.

C. Electronic Configuration and Equilibrium Geometries of TiH_2·H_2, VH_2·H_2, and CrH_2·H_2. I. TiH_2·H_2. For MH_2·H_2 complexes, including TiH_2·H_2, VH_2·H_2, and CrH_2·H_2, three arrangements in C_{2v} symmetry are considered routinely:

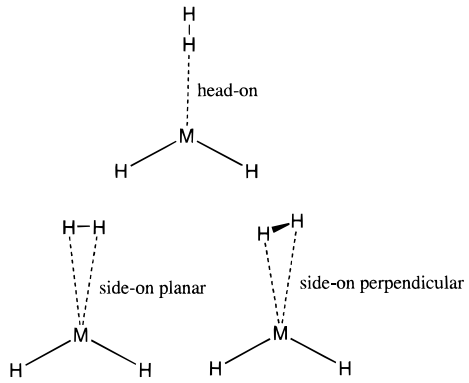

The three lowest lying electron configurations of TiH_2 are $6a_1{}^2 3b_2{}^2 7a_1 1a_2$, $6a_1{}^2 3b_2{}^2 7a_1 8a_1$, and $6a_1{}^2 3b_2{}^2 7a_1 3b_1$. Thus, for each of the TiH_2·H_2 arrangements we investigated three electronic configurations, i.e., $7a_1{}^2 3b_2{}^2 8a_1 1a_2$, $7a_1{}^2 3b_2{}^2 8a_1 9a_1$, and $7a_1{}^2 3b_2{}^2 7a_1 3b_1$, leading to $^3A_2$, $^3A_1$, and $^3B_1$ electronic states, respectively. However, we found that the C_{2v} potential energy surfaces for all three arrangements are repulsive between the TiH_2 and H_2 fragments, leading to more than 3.5 Å separation between the two fragments (supporting information, Table 7). TiH_2 and H_2 are attractive on the potential energy surface with C_s symmetry, as indicated in Figure 2a. TiH_2·H_2 thus has a $^3A''$ ground electronic state, which is formed by the H_2 molecule and the TiH_2 molecule in its $^3B_1$ ground electronic state. The dihydrogen bonding energy for TiH_2·H_2 was predicted to be 1.7 kcal mol^{-1} at the TZP CCSD level of theory and 2.8 kcal mol^{-1} at the TZP(f,d) CCSD(T) level of theory:

$$TiH_2(^3B_1) + H_2 \rightarrow TiH_2{\cdot}H_2\ (^3A'') \qquad \Delta E = -2.8 \text{ kcal mol}^{-1} \quad (1)$$

A possible closed shell singlet TiH_2·H_2 was also sought. However, on the singlet potential energy surface, the H_2 moiety dissociates without a barrier and optimization leads to the titane molecule (TiH_4). Therefore, the TiH_2·H_2 species does not exist on the low-spin potential energy surface.

II. VH_2·H_2. As for the TiH_2·H_2, we investigated the side-on planar and side-on ortho conformations for VH_2·H_2 with the various electronic states. The head-on conformation for VH_2·H_2 was tested with the electronic configuration $7a_1{}^2 3b_2{}^2 8a_1 1a_2 3b_1$, which originates from the ground $^4B_2$ state of VH_2. It was found that with the $7a_1{}^2 3b_2{}^2 8a_1 1a_2 3b_1$ electronic configuration, the potential energy surfaces for all three arrangements were repulsive between VH_2 and H_2.

With the $7a_1{}^2 3b_2{}^2 8a_1 4b_2 3b_1$ electronic configuration ($^4A_2$), VH_2 and H_2 are attractive in both the side-on planar and the side-on ortho conformation, with the side-on planar conformation being lower in energy (Figure 1e and supporting information, Table 7). Both the $^4A_2$ and $^4\Pi_g$ stages of VH_2 (Table 2) may lead to the $^4A_2$ state of VH_2·H_2. However, the nearly linear VH_2 fragment in the $^4A_2$ state of VH_2·H_2 (Figure 1d) suggests that the $^4A_2$ state of VH_2·H_2 is formed from the $^4\Pi_g$ state of VH_2. In the C_s symmetry conformation (Figure 1c), the $^4A_2$ state of VH_2 (Table 2) lead to the $^4A''$ electronic state of VH_2·H_2, which is the ground state. The H_2 moiety positions itself directly above the VH_2 plane in this global minimum structure (Figure 1c).

We have also investigated the side-on planar and side-on ortho conformations of VH_2·H_2 on the low-spin potential energy surface. Both the $7a_1{}^2 3b_2{}^2 3b_1{}^2 8a_1$ and $7a_1{}^2 3b_2{}^2 3b_1{}^2 1a_2$ electronic configurations have been considered. The former configuration originates from the $^2A_1$ state of VH_2 ($6a_1{}^2 3b_2{}^2 3b_1{}^2 7a_1$), which is the lowest state on the low-spin potential energy surface. The $7a_1{}^2 3b_2{}^2 3b_1{}^2 1a_2$ electronic configuration is important for studing the formation of the VH_4 molecule, whose ground electronic state has the $7a_1{}^2 3b_2{}^2 3b_1{}^2 1a_2$ electronic configuration in C_{2v} symmetry.

Unlike the low-spin TiH_2·H_2, the low-spin VH_2·H_2 does correspond to a minimum on the potential energy surface. On the low-spin potential energy surfaces, VH_2 and H_2 are strongly attractive, with the side-on ortho conformation being lower in energy. The H_2 moiety for low-spin VH_2·H_2 is strongly activated in the side-on ortho conformation with $7a_1{}^2 3b_2{}^2 3b_1{}^2 1a_2$ electronic configuration (supporting information, Table 7). The Jahn−Teller effect occurs here. The side-on ortho conformation in the $^2A_1$ state was a transition state to a lower C_s symmetry conformation (Figure 1d). The doublet VH_2·H_2 has C_s symmetry and the symmetry plane contains the H_2 moiety and bisects the VH_2 angle (Figure 1d). The interaction between the H_2 and VH_2 moieties is very strong in this $^2A''$ state. The H−H distance is elongated to 0.831 Å and has a shorter V···H_2 distance than for the $^4A''$ global minimum state. Despite structural sensitivity to basis set, the dihydrogen bonding energies for VH_2·H_2 are almost identical at the TZP CCSD and TZP(f,d) CCSD levels of theory, indicating a good energetic convergence. The binding energy between the two moieties is much higher in the low-spin state than in the high-spin state, as indicated by the exothermicities for the following reactions at the TZP(f,d) CCSD(T) level of theory:

$$VH_2\ (^2A_2) + H_2 \rightarrow VH_2{\cdot}H_2\ (^2A'') \qquad \Delta E = -22.4 \text{ kcal mol} \quad (2)$$

$$VH_2\ (^4B_2) + H_2 \rightarrow VH_2{\cdot}H_2\ (^4A'') \qquad \Delta E = -7.1 \text{ kcal mol}^{-1} \quad (3)$$

III. CrH_2·H_2. We investigated the side-on planar and side-on ortho conformations of CrH_2·H_2 with different electron configurations. Ground state CrH_2 ($^5B_2$) was found to be weakly repulsive with respect to attachment of an H_2 molecule for both planar and ortho conformations (supporting information, Table 7). However, in the linear $^5A_1$ state, CrH_2 does attract the H_2

molecule. The side-on planar conformation with the $7a_1{}^2 3b_2{}^2 8a_1 3b_1 1a_2 4b_2$ electronic configuration was found to be the ground state for the $CrH_2{\cdot}H_2$ complex (Figure 2b). The CrH_2 moiety is still close to linear (176.3°) in the $^5A_1$ ground state of $CrH_2{\cdot}H_2$. The side-on ortho conformation with the $7a_1{}^2 3b_2{}^2 8a_1 3b_1 1a_2 4b_2$ electronic configuration is a transition state for the H_2 rotation. The rotation barrier was found to be 2.1 kcal mol^{-1} at the TZP CISD level of theory.

On the low-spin potential energy surface, the interaction between the CrH_2 and H_2 fragments is fairly strong. We investigated the side-on ortho conformation with both the $7a_1{}^2 3b_2{}^2 3b_1{}^2 4b_1 1a_2$ and the $7a_1{}^2 3b_2{}^2 3b_1{}^2 8a_1 1a_2$ electronic configurations (supporting information, Table 7). The former configuration originates from the $^3B_2$ state of CrH_2, which is the lowest lying state on the low-spin potential energy surface. It is important to compare the latter configuration ($^3A_1$) with the CrH_4 molecule, which has the same electronic configuration in C_{2v} symmetry. The $^3B_2$ state $CrH_2{\cdot}H_2$ is a transition state with respect to the rotation of the H_2 moiety. Finally, we found that a C_2 symmetry $CrH_2{\cdot}H_2$ structure with the ^3B electronic state is the lowest in energy on the low-spin potential energy surface (Figure 2c). Similar to the case of $VH_2{\cdot}H_2$, the interaction between the H_2 and CrH_2 moieties is stronger on the low-spin potential energy surface (^3B) than on the high-spin ($^5A_1$) potential energy surface. The H−H bond (0.776 Å) is longer and the $H_2{\cdots}CrH_2$ distance (1.805 Å) is shorter in the ^3B state than for the $^5A_1$ state (0.753 and 2.058 Å, respectively). The binding energy between H_2 and CrH_2 parallel to that of the $VH_2{\cdot}H_2$ system at the TZP(f,d) CCSD(T) level of theory is given by:

$$CrH_2\ (^3A_2) + H_2 \rightarrow CrH_2{\cdot}H_2\ (^3B) \qquad \Delta E = -15.5\ \text{kcal mol}^{-1} \quad (4)$$

$$CrH_2\ (^5A_1) + H_2 \rightarrow CrH_2{\cdot}H_2\ (^5A_1) \qquad \Delta E = -3.1\ \text{kcal mol}^{-1} \quad (5)$$

4. Discussion

A. Periodic Trends for MH_2 Molecules and $MH_2{\cdot}H_2$ Complexes I. MH_2 Molecules. Even though the bonding in the cationic species essentially involves the valence s and d orbitals on the transition metal, the p orbitals also participate in the case of the neutral species. Previous SCF studies indicated that the 3d contribution to the MH_2 bonding should be strong for the three early elements of the first transition metal series (Ti, V, and Cr)[5,7] even though at the SCF level, the $3d_M-1s_H$ interaction is still too weak to overcome the $4sp_M-1s_H$ mixing which dominates the bonding scheme and determines the linear geometry. However, with electron correlation effects included, the $3d_M-1s_H$ interaction becomes more important and TiH_2, VH_2, and CrH_2 all have bent equilibrium structures on the high-spin potential energy surfaces. The bond angles decrease from TiH_2 via VH_2 to CrH_2, i.e., 142.1°, 138.8°, and 121.8°, respectively, at the TZP(f,d) CISD level of theory (Tables 1−3), indicating increasing $3d_M-1s_H$ interaction in the M−H bonding. This is reasonable. For example, the Cr atoms has a $3d^5 4s$ ground state. To form CrH_2, one of the d orbitals has to be involved in M−H bonding. However, it should be kept in mind that the $3d_M-1s_H$ interaction is still very weak in the absolute sense. The potential energy surfaces are very flat and the energy difference between linear and bent structures is very small. This is the main reason why the MH_2 bond angles in TiH_2, for instance, are sensitive to the basis set.

As can be seen from Figure 3, the energy separation between the high-spin ground state and the lowest low-spin state for isolated MH_2 molecules increases from right to left in the periodic table: 33 kcal mol^{-1} for TiH_2, 40 kcal mol^{-1} for VH_2, and 59 kcal mol^{-1} for CrH_2. This trend is important in understanding the relative energy between $MH_2{\cdot}H_2$ and the MH_4 isomers. We will come back to this topic in the next section.

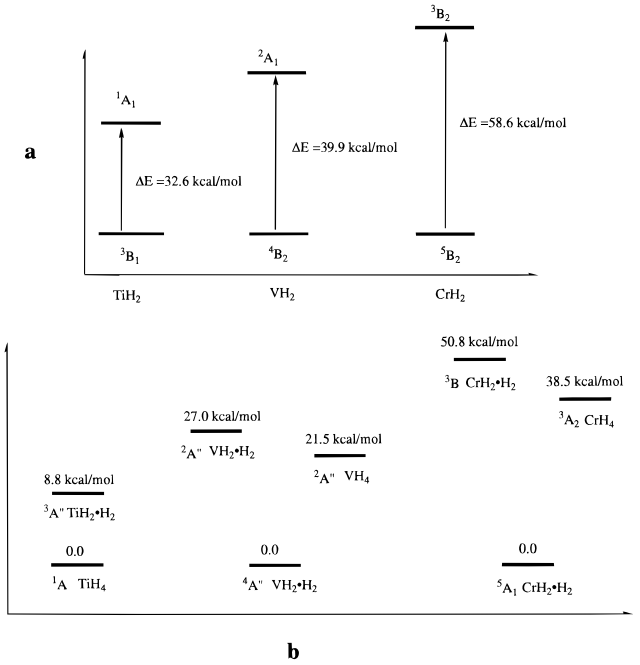

Figure 3. (a) The energy separations between the ground states and the lowest lying low-spin states for the MH_2 molecules at the TZP CCSD level of theory. (b) The energy separations between the $MH_2{\cdot}H_2$ and MH_4 isomers at the TZP CCSD level of theory.

II. $MH_2{\cdot}H_2$. We have mentioned the dihydrogen binding energy in the $MH_2{\cdot}H_2$ complexes in previous sections; we list those reactions here to show the periodic trend.

$$TiH_2\ (^3A_1) + H_2 \rightarrow TiH_2{\cdot}H_2\ (^3A'') \qquad \Delta E = -2.8\ \text{kcal mol}^{-1} \quad (1)$$

$$VH_2\ (^2A_1) + H_2 \rightarrow VH_2{\cdot}H_2\ (^2A'') \qquad \Delta E = -22.4\ \text{kcal mol}^{-1} \quad (2)$$

$$VH_2\ (^4A_2) + H_2 \rightarrow VH_2{\cdot}H_2\ (^4A'') \qquad \Delta E = -7.1\ \text{kcal mol}^{-1} \quad (3)$$

$$CrH_2\ (^3B_2) + H_2 \rightarrow CrH_2{\cdot}H_2\ (^3B) \qquad \Delta E = -15.5\ \text{kcal mol}^{-1} \quad (4)$$

$$CrH_2\ (^5A_1) + H_2 \rightarrow CrH_2{\cdot}H_2\ (^5A_1) \qquad \Delta E = -3.1\ \text{kcal mol}^{-1} \quad (5)$$

For the high-spin species the H_2 bond lengths are 0.758, 0.761, and 0.758 Å for the $^3A''$ state of $TiH_2{\cdot}H_2$, $^4A''$ state of $VH_2{\cdot}H_2$, and $^5A_1$ state of $CrH_2{\cdot}H_2$, respectively. On the low-spin potential energy surfaces, the d → σ^* back-donation is so strong for the $TiH_2 + H_2$ system that the H_2 bond breaks without barrier upon forming the complex with singlet TiH_2, subsequently forming TiH_4. The H_2 bond length is 0.831 Å in the $^2A''$ state of $VH_2{\cdot}H_2$, indicating a significant activation of the H_2 molecule. However, the H_2 bond distance is only 0.776 Å in the ^3B state of $CrH_2{\cdot}H_2$ (Figure 2c, C_2 symmetry).

It may be seen that the binding energy involving the low-spin MH_2 complexes is substantially higher than that of the high-spin species and the binding energies decrease with increasing atomic number. The stronger dihydrogen bonding in the low-

spin state is not surprising. It was found experimentally[16] that the high-spin transition metal ions prevent bonding with the hydrogen molecule and the H_2 is activated more strongly by the atomic transition-metal ion in the low-spin state. This may be explained in terms of d $\rightarrow \sigma^*$ back-donation. By chemical intuition, the ability for electron donation from d orbitals is expected to decrease from the right to the left in the periodic table, because the 3d orbitals penetrate the electron density in the 4s orbitals; therefore, the effective nuclear charges experienced by the 3d orbitals increase rather abruptly from the right to the left in the periodic table. For effective d $\rightarrow \sigma^*$ back-donation to occur, the d electrons should be paired, i.e., in the low-spin state. It has been shown in the case of cationic species that the loss of exchange energy during the bond formation is a very important factor. This argument may also explain the favored "two-electron" versus "one-electron" back-donation.

There is a hotly debated question concerning the nature of the dihydrogen complexes. The barrier to rotation about the M−H_2 axis may be used to tell whether d(π) $\rightarrow \sigma^*$ back-bonding is important. For the high-spin $MH_2{\cdot}H_2$ complexes, we found that the rotation barriers are around 1 to 2 kcal/mol. However, for the low-spin state of $VH_2{\cdot}H_2$ (electron configuration: $7a_1^2 3b_2^2 3b_1^2 1a_2$, supporting information, Table 3), the energy difference between the side-on planar and perpendicular conformations is as large as 18 kcal/mol at the TZP CCSD level, indicating a large rotation barrier and a strong d(π) $\rightarrow \sigma^*$ back bonding. Unambiguous evidence for the d $\rightarrow \sigma^*$ back bonding has been obtained by examination of the molecular orbitals for the dihydrogen complexes. For the low-spin states $VH_2{\cdot}H_2$ ($^2A''$) and $CrH_2{\cdot}H_2$ (^3B), there is very strong d $\rightarrow \sigma^*$ back bonding, as is the case for genuine chemical bonds (Figure 4); this back-bonding is absent in the molecular orbitals of the high-spin $MH_2{\cdot}H_2$ complexes.

It is important to note that the triplet ground state of TiH_2 leads to the formation of the triplet ground state of the $TiH_2{\cdot}H_2$ complex. By contrast, the formation of the ground states of the $VH_2{\cdot}H_2$ and $CrH_2{\cdot}H_2$ complexes arise from the $^4A_2$ state of VH_2 and the $^5A_1$ state of CrH_2, respectively. Note that both $^4A_2$ VH_2 and $^5A_1$ CrH_2 are excited electronic states, even though they are very close to the ground state energetically. Therefore, we predict that $TiH_2{\cdot}H_2$ will be readily formed whenever TiH_2 is in contact with H_2 molecules, whereas $VH_2{\cdot}H_2$ and $CrH_2{\cdot}H_2$ will be formed only when VH_2 and CrH_2 are energetically excited, for example by photolysis. This prediction is important in the assignment of experimental IR spectra[4] and in the identification of the possible formation of $TiH_2{\cdot}H_2$, $VH_2{\cdot}H_2$, and $CrH_2{\cdot}H_2$. We will discuss this topic in the final section.

III. The Relative Energies of $MH_2{\cdot}H_2$ Complexes and Their MH_4 Isomers. Quantification of the energy separations between the $MH_2{\cdot}H_2$ structures and their MH_4 isomers is crucial to a proper description of the dihydrogen complex/hydride interconversion. As may be seen from Figure 3b, TiH_4 is lower in energy than its dihydrogen complex isomer $TiH_2{\cdot}H_2$, whereas VH_4 and CrH_4 are higher in energy than their dihydrogen complex (high-spin global minima) isomers by 21.5 and 38.5 kcal mol^{-1}, respectively. However, comparing an MH_4 molecule and a $MH_2{\cdot}H_2$ complex at the same spin state, on the low-spin potential energy surface, the MH_4 molecule is always lower in energy than the dihydrogen complex isomer $MH_2{\cdot}H_2$.

As may be seen from Figure 3a, the energy separations between the high-spin and low-spin isolated MH_2 molecules increase with the atomic number: 33 kcal mol^{-1} for TiH_2, 40 kcal mol^{-1} for VH_2, and 59 kcal mol^{-1} for CrH_2. Because the H_2 binds more strongly to the low-spin MH_2, the energy separation between high-spin and low-spin $MH_2{\cdot}H_2$ complexes narrows slightly. For the $MH_2{\cdot}H_2$ complexes the energy separations between the high-spin states and the comparable low-spin states are still large: 27 kcal mol^{-1} for $VH_2{\cdot}H_2$ and 50.8 kcal mol^{-1} for $CrH_2{\cdot}H_2$. Therefore, we expect that the low-spin MH_4 would be higher in energy than the high-spin $MH_2{\cdot}H_2$, unless the isomerization from low-spin $MH_2{\cdot}H_2$ to MH_4 is very exothermic, as in the case of isomerization from $TiH_2{\cdot}H_2$ to TiH_4.

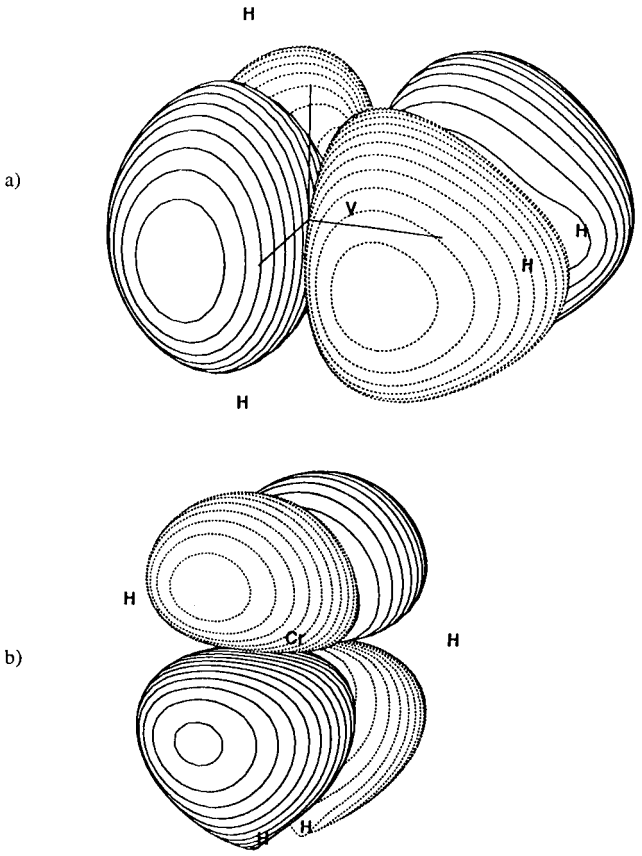

Figure 4. (a) The contour map of the 10a″ orbital (d $\rightarrow \sigma^*$ back bonding) of $^2A''$ $VH_2{\cdot}H_2$ (point group C_s). (b) The contour map of the 5b orbital (d $\rightarrow \sigma^*$ back bonding) of ^3B $CrH_2{\cdot}H_2$ (point group C_2).

Experiments have been performed for all three light transition metals (Ti, V, and Cr) in cocondensation with H_2. Experimentally,[4] only TiH_4 has been observed in the lab,[4] whereas VH_4 and CrH_4 remain elusive. The reason that TiH_4 is easily formed is perhaps obvious−it is lower in energy than $TiH_2{\cdot}H_2$. However, note that a spin flip must occur to form MH_4 from either a MH_2 molecule or a $MH_2{\cdot}H_2$ complex, since the fomer has a low-spin ground state, whereas the latter two have high-spin ground states. Therefore, the facile spin flip of the Ti system must be another important factor that facilitates the formation of the TiH_4 molecule. Both the $^2A_2$ ground state of VH_4 and the $^3A_2$ ground state of CrH_4 have been proven by vibrational frequency analysis to be true minima on the potential energy surfaces (VH_4, see section 1, this work; CrH_4, see ref 15). Both VH_4 and CrH_4 are lower in energy than the low-spin isomers $VH_2{\cdot}H_2$ and $CrH_2{\cdot}H_2$, respectively. Following the same arguments regarding the spin flip, provided that the low-spin species of MH_2 or $MH_2{\cdot}H_2$ (here M = V, Cr) could be obtained, it is probable that both VH_4 and CrH_4 could be formed as well.

B. Comparison between Theoretical and Experimental IR Spectra for the TiH_2, VH_2, and $CrH_2{\cdot}H_2$ Systems. I. TiH_2 or $TiH_2{\cdot}H_2$? For the TiH_2 molecule, comparison between our theoretical vibrational frequencies and experimental IR spectra[4] is challenging. At first sight, the agreement is very poor (Table 4). There are two possible factors responsible for this discrepancy.

Table 4. harmonic Vibrational Frequencies and IR Intensities for $^3B_1$ TiH_2 at the TZP CISD and TZP(f,d) CISD Levles of Theory[a]

	TiH_2				TiDH				TiD_2			
	this work			expt[c]	this work			expt[b]	this work			expt[b]
mode	ω (cm^{-1})	ω (cm^{-1}) scaled[a]	IR intensity (km/mol)	ω (cm^{-1})	ω (cm^{-1})	ω (cm^{-1}) scaled[a]	IR intensity (km/mol)	ω (cm^{-1})	ω (cm^{-1})	ω (cm^{-1}) scaled[a]	IR intensity (km/mol)	ω (cm^{-1})
symm	1611	1530	215	1478[d]	1154	1096	198	1039[d]	1142	1084	47	1058[d]
stretch	**1612**	**1531**	**198**	1483[e]	**1154**	**1096**	**239**	1055[e]	**1143**	**1084**	**81**	1071[e]
asymm	1609	1528	537	1412[d]	1612	1531	374	1447[d]	1164	1105	345	1024[d]
stretch	**1604**	**1523**	**692**	1435[e]	**1609**	**1528**	**438**	1466[e]	**1161**	**1103**	**383**	1041[e]
bend	326	309	341	496[d]	284	270	260		235	233	176	376[d]
	375	**356**	**319**		**326**	**309**	**244**		**269**	**255**	**165**	

[a] The values in plain text are at the TZP CISD level of theory and the values in boldface are at the TZP(f,d) CISD level of theory. [b] The vibrational frequencies were scaled by a factor of 0.95 to account for anharmonicity and higher level correlation effects. [c] Reference 4. [d] In Kr matrix. [e] In Ar matrix.

Table 5. Harmonic Vibrational Frequencies and IR Intensities for $^3A''$ $TiH_2{\cdot}H_2$ at the TZP CISD Level of Theory

		$TiH_2{\cdot}H_2$			$TiD_2{\cdot}D_2$		
no.	mode	ω (cm^{-1})	ω (cm^{-1}) scaled[a]	IR intensity (km/mol)	ω (cm^{-1})	ω (cm^{-1}) scaled[a]	IR intensity (km/mol)
1	H−H stretch	4139	3932	64	2928	2781	32
2	H−Ti−H symm stretch	1586	1506	218	1116	1060	164
3	H−Ti−H asymm stretch	1558	1480	553	1131	1074	238
4	Ti···H−H wag	958	910	7.9	679	646	4
5	H−Ti−H bend	520	494	274	375	356	136
6	H−Ti···H bend	467	443	36	331	314	20
7	Ti···H−H torsion	380	361	76	271	257	42
8	H−Ti−H bend	327	310	248	238	226	128
9	Ti···H−H wag	252	239	64	181	171	32

[a] The vibrational frequencies were scaled by a factor of 0.95 to account for anharmonicity and higher level correlation effects.

Table 6. Harmonic Vibrational Frequencies and IR Intensities for $^4B_2$ VH_2 at the TZP CISD and TZP(f,d) CISD Levels of Theory[a]

	VH_2				VDH				VD_2			
	this work			expt[c]	this work			expt[b]	this work			expt[b]
mode	ω (cm^{-1})	ω (cm^{-1}) scaled[a]	IR intensity (km/mol)	ω (cm^{-1})	ω (cm^{-1})	ω (cm^{-1}) scaled[a]	IR intensity (km/mol)	ω (cm^{-1})	ω (cm^{-1})	ω (cm^{-1}) scaled[a]	IR intensity (km/mol)	ω (cm^{-1})
symm	1643	1550	47	1545[d]	1158	1100	211	1095[d]	1165	1107	25	1079[d]
stretch	**1670**	**1586**	**67**	1532[e]	**1174**	**1115**	**236**	1108[e]	**1186**	**1127**	**36**	1092[e]
asymm	1597	1517	681	1490[d]	1621	1540	343	1518[d]	1151	1093	357	1111[d]
stretch	**1612**	**1531**	**724**	1508[e]	**1643**	**1561**	**366**	1536[e]	**1161**	**1103**	**379**	1123[e]
bned	322	306	418	529[e]	280	266	320		231	220	217	386[d]
	368	**350**	**379**		**320**	**304**	**291**		**264**	**251**	**196**	

[a] The values in plain text are at the TZP CISD level of theory and the values in boldface are at the TZP(f,d) CISD level of theory. [b] The vibrational frequencies were scaled by a factor of 0.95 to account for anharmonicity and higher level correlation effects. [c] Reference 4. [d] In Kr matrix. [e] In Ar matrix.

1. Experiments[4] show that the MH_2 stretching vibrational frequencies are sensitive to the polarizability of the matrix. An increase in the polarizability of the matrix decreases the magnitude of the vibrational frequencies. This effect increases from $TiH_2{\cdot}H_2$ to $VH_2{\cdot}H_2$ to $CrH_2{\cdot}H_2$. For example, the asymmetric stretching frequencies for CrH_2 are 1614 cm^{-1} in the Ar matrix and 1606 cm^{-1} in the Kr matrix; for VH_2, 1508 cm^{-1} in Ar and 1490 in Kr; and for TiH_2, 1436 cm^{-1} in Ar and 1412 in Kr. These shifts correspond to −8, −18, and −24 cm^{-1} for TiH_2, VH_2, and CrH_2, respectively. This could be one reason that our scaled vibrational frequencies for the TiH_2 molecule are 50 and 110 cm^{-1} higher than experimental assignments for symmetrical and asymmetrical stretching, respectively. Whereas experiment predicts that the asymmetrical stretch is 50 cm^{-1} lower than the symmetrical stretching for TiH_2, theory predicts an 8-cm^{-1} separation. This discrepancy may indicate that the asymmetrical stretch is more sensitive to the matrix environment.[4]

2. Secondly, the poor agreement may be a consequence of the possible formation of the $TiH_2{\cdot}H_2$ complex. Recall that the $TiH_2{\cdot}H_2$ complex could be formed as long as TiH_2 was allowed to come in contact with the H_2 molecule. If the $TiH_2{\cdot}H_2$ complex (or its deuterated species) forms following the formation of TiH_2, the experimental IR absorption may be due to $TiH_2{\cdot}H_2$ rather than TiH_2. Three observations (Table 5) support this hypothesis, i.e., (I) the H−Ti−H stretching frequencies are much lower for the $TiH_2{\cdot}H_2$ complex than for the isolated TiH_2 molecule, making the predictions for $TiH_2{\cdot}H_2$ agree more closely with the experimental IR absorption; (II) the separation between symmetric and asymmetric H−Ti−H stretching frequencies is larger for $TiH_2{\cdot}H_2$ (28 cm^{-1}) than for the isolated TiH_2 molecule (8 cm^{-1}), making the predictions for $TiH_2{\cdot}H_2$ agree more closely with the experimental IR absorption; and (III) the experimental IR absorption for the H−Ti−H bending mode (496 cm^{-1}) is 160 cm^{-1} higher than the corresponding theoretical value (356 cm^{-1}, scaled, Table 4). By contrast, the H−Ti−H bending mode (or Ti···H_2 wag) in $TiH_2{\cdot}H_2$ at 494 cm^{-1} is in excellent agreement with the experimental absorption. This fact gives support to our suggestion that the observed species is $TiH_2{\cdot}H_2$ rather than TiH_2. Experimentally, the IR spectra of the Ti_xH_y systems were sensitive to the Ti concentration, and a low Ti concentration was used. When a high Ti concentration was used, there was a strong broad absorption around 1500 cm^{-1}. This broad peak was thought to result from a spontanous reaction of the Ti_2 or Ti_3 clusters with H_2. However, it is

Table 7. Harmonic Vibrational Frequencies and IR Intensities for $^4A''$ $VH_2 \cdot H_2$ at the TZP CISD and TZP(f,d) CISD Levels of Theory[a]

		$VH_2 \cdot H_2$			$VD_2 \cdot D_2$		
no.	mode	ω (cm^{-1})	ω (cm^{-1}) scaled[b]	IR intensity (km/mol)	ω (cm^{-1})	ω (cm^{-1}) scaled[b]	IR intensity (km/mol)
1	H−H stretch	4157	3949	3	2940	2793	1
		4232	**4020**	**4**	**2993**	**2843**	**2**
2	H−V−H symm stretch	1654	1571	29	1172	1060	15
		1674	**1590**	**43**	**1187**	**1127**	**24**
3	H−V−H asymm stretch	1600	**1520**	**774**	**1152**	**1094**	**399**
4	V···H_2 rock	1050	997	5	743	705	3
		1081	**1026**	**5**	**769**	**730**	**3**
5	V···H_2 wag	551	523	4	400	380	8
		577	**548**	**8**	**418**	**397**	**11**
6	V···H_2 torsion	462	438	0	327	310	0
		455	**432**	**2**	**322**	**306**	**1**
7	V···H_2 wag	445	422	452	318	302	228
		435	**413**	**462**	**311**	**295**	**232**
8	H−V−H bend	268	254	7	191	181	3
		283	**269**	**7**	**203**	**192**	**4**
9	V···H_2 wag	232	220	498	167	158	257
		253	140	**457**	**180**	**171**	**235**

[a] The values in plain text are at the TZP CISD level of theory and those in boldface are at the TZP(f,d) CISD level of theory. [b] The vibrational frequencies were scaled by a factor of 0.95 to account for anharmonicity and higher level correlation effects.

Table 8. Harmonic Vibrational Frequencies and IR Intensities for $^5A_1 CrH_2 \cdot H_2$ at the TZP CISD Level of Theory

		$CrH_2 \cdot H_2$			$CrD_2 \cdot D_2$		
no.	mode	ω (cm^{-1})	ω (cm^{-1}) scaled[a]	IR intensity (km/mol)	ω (cm^{-1})	ω (cm^{-1}) scaled[a]	IR intensity (km/mol)
1	H−H stretch	4286	4071	0	3032	2880	0
2	H−Cr−H symm stretch	1723	1636	10	1219	1060	5
3	H−Cr−H asymm stretch	1606	1525	862	1157	1102	443
4	Cr···H−H bend	996	946	6	705	670	4
5	Cr···H−H bend	523	497	430	379	360	213
6	H−Cr···H bend	495	470	370	356	338	191
7	Cr···H_2 stretch	473	449	7	337	320	15
8	H−Cr···H bend	466	442	0	329	312	0
9	H−Cr···H bend	351	333	10	250	337	6

[a] The vibrational frequencies were scaled by a factor of 0.95 to account for anharmonicity and higher level correlation effects.

possible that this broad peak results from TiH_2, which is favored at a high Ti/H_2 ratio.

II. VH_2 and $VH_2 \cdot H_2$? For the VH_2 molecule, it seems that our theoretical harmonic vibrational frequencies for the stretching modes agree with experimental assignments fairly well. However, when the possible existence of $VH_2 \cdot H_2$ is taken into consideration, the situation becomes more complex. The problem is that the H−V−H stretching frequencies for the VH_2 molecule and the $VH_2 \cdot H_2$ complex (Tables 6 and 7) are very close. From the analysis in the previous sections, we predict that the $VH_2 \cdot H_2$ complex is formed from H_2 with an excited VH_2 molecule. Therefore, $VH_2 \cdot H_2$ may coexist with the ground state of VH_2 after photolysis of the matrix, although it is difficult to deduce the concentration ratio. There are some less intense side bands with the same vibrational modes in the experimental IR spectra.[4] Xiao et al.[4] attributed these bands to different matrix sites. However, it may be more plausible that the bands are due to either VH_2 or $VH_2 \cdot H_2$.

Comparing the theoretical vibrational frequency to the experimental assignment for the VH_2 bending, it seems evident that $VH_2 \cdot H_2$ was formed. Our theoretical value for the VH_2 bending is 350 cm^{-1}, whereas the experimental absorption falls at 529 cm^{-1}. However, as may be seen from Table 8, the experimental 529-cm^{-1} absorption is probably due to the V···H_2 wag for the $VH_2 \cdot H_2$ complex, which is predicted to be 548 cm^{-1} at the TZP(f,d) CISD level of theory.

The 1995 ESR experiments by Van Zee, Li, and Weltner[4b] may indicate that the VD_2 molecule interacts with D_2 in the deuterium matrix. Van Zee concluded that the VD_2 molecule is nearly linear in the deuterium matrix, in contrast to our theoretical results (Table 2) and the experimental IR results.[4a] One explanation of such a difference is that VD_2 interacts with D_2 more strongly in the linear than in the bent conformation to form $VD_2 \cdot (D_2)_n$. We predict a $^4A_2$ state $VH_2 \cdot H_2$ (Figure 1d), in which the VH_2 fragment is nearly linear. This $^4A_2$ state lies only 1.5 kcal mol^{-1} higher in energy than the $^4A''$ ground state $VH_2 \cdot H_2$ (Figure 1b), in which the VH_2 fragment is bent. Therefore, it may be possible that VD_2 is nearly linear in the deuterium matrix.

III. $CrH_2 \cdot H_2$. Of the three possible dihydride dihydrogen complexes, namely $TiH_2 \cdot H_2$, $VH_2 \cdot H_2$, and $CrH_2 \cdot H_2$, only $CrH_2 \cdot H_2$ is thought to have been observed experimentally.[4a] However, it seems that the original identification was erroneous. The comparison of our theoretical vibrational frequencies for $CrH_2 \cdot H_2$ ($CrD_2 \cdot D_2$) with the experimentally assigned spectra for CrH_2, CrH_3, and $CrH_2 \cdot H_2$ (and their corresponding deuterated species) reveals an important discrepancy. Based on the observation of the double peaks in the range of 1640 to 1606 cm^{-1}, Xiao et al. proposed the formation of $CrH_2 \cdot H_2$. Further, a very strong absorption in 1510 cm^{-1} was assigned to CrH_3 by Xiao et al.[4] However, as can be seen in Table 8, this 1510-cm^{-1} absorption belongs unambiguously to the asymmetrical stretch of $CrH_2 \cdot H_2$. The double peaks in the range of 1640 to 1606 cm^{-1} could be due to matrix site effects. Actually, the 1621- and 1579-cm^{-1} absorptions, previously assigned to $CrH_2 \cdot H_2$, were observed in the Kr matrix only and no such absorption was observed in the Ar matrix. By contrast, the 1510-cm^{-1} absorption was observed in both matrices. This finding is more consistent with the idea that $CrH_2 \cdot H_2$ should be formed independent of the host matrix.

5. Conclusions

We have investigated the structures and potential energy surfaces for transition metal dihydrides, MH_2, dihydride dihydrogen complexes, $MH_2{\cdot}H_2$, and tetrahydrides, MH_4, (M = Ti, V, and Cr). The ground electronic states for TiH_2 and VH_2 were found to be $^3B_1$ and $^4B_2$, respectively. The bond angles for the TiH_2 and VH_2 molecules are predicted to be 142° and 138.8°, respectively, at the TZP(f,d) CISD level of theory. On the low-spin potential energy surfaces, the lowest lying electronic states for the TiH_2, VH_2, and CrH_2 molecules are $^1A_1$, $^2A_1$, and $^3B_2$, respectively. The energy separations between the ground state and the lowest lying low-spin state were found to be 33, 40, and 59 kcal mol^{-1} for the TiH_2, VH_2, and CrH_2 molecules, respectively. The ability to form dihydrogen complex decreases with increasing atomic number. The d $\rightarrow \sigma^*$ back-donation dominates the periodic trend for the formation of $MH_2{\cdot}H_2$ complexes. All three $MH_2{\cdot}H_2$ complexes have high-spin ground states, primarily due to the fact that the corresponding parent dihydrides are in the high-spin ground state. It was found that the low-spin dihydrides interacted with the H_2 moiety more strongly than did the high-spin species. The d $\rightarrow \sigma^*$ back-donation was so strong for the low-spin TiH_2 that H_2 dissociates without barrier upon contact with singlet TiH_2 to form TiH_4. The energy separations between the ground state and the lowest lying low-spin state were 27 and 51 kcal mol^{-1} for $VH_2{\cdot}H_2$ and $CrH_2{\cdot}H_2$, respectively. The dihydrogen binding energies were evaluated to be 2.8 kcal mol^{-1} for the high-spin TiH_2, 7.1 and 22.4 kcal mol^{-1} for the high-spin and the low-spin VH_2, respectively, and 3.1 and 15.5 kcal mol^{-1} for the high-spin and the low-spin CrH_2, respectively, at the TZP(f,d) CCSD(T) level of theory.

The VH_4 molecule is predicted to have D_{2d} symmetry with a bond length of 1.622 Å and bond angles distorted from the tetrahedral 109.5° to 114.1° and 100.5° at the TZP(f,d) CISD level of theory (Figure 1a). The ground state electron configuration for the VH_4 molecule was $1a_1^2 2a_1^2 1b_1^2 1e^4 3a_1^2 2b_1^2 2e^4 4a_1^2 3b_1^2 3e^4 5a_1$, leading to the $^2A_1$ electronic state.

Closed-shell TiH_4 is 9 kcal mol^{-1} lower in energy than its triplet ground state $MH_2{\cdot}H_2$ isomer, whereas VH_4 and CrH_4 are higher in energy by 22 and 39 kcal mol^{-1}, respectively, at the TZP CCSD level of theory. However, comparing MH_4 and $MH_2{\cdot}H_2$ in the same spin state, MH_4 is always lower in energy than its dihydrogen complex isomer, $MH_2{\cdot}H_2$, on the low-spin potential energy surface.

Comparison between the present work and the experimental matrix isolation IR spectra from the cocondensation of transition metal atoms (Ti, V, and Cr) with H_2 appears to confirm the existence of $CrH_2{\cdot}H_2$ by identifying a strong unique absorption at 1510 cm^{-1}. It is suggested that $TiH_2{\cdot}H_2$ rather than TiH_2 may be observed experimentally, and that $VH_2{\cdot}H_2$ may be formed concomitently with the VH_2 molecule.

Acknowledgment. We thank Drs. Y. Xie, Y. Yamaguchi, J. R. Thomas, and B. J. Deleeuw for helpful discussions. This research was supported by the U.S. Department of Energy, Office of Basic Energy Sciences, Division of Chemical Sciences, Fundamental Interactions Branch, Grant No DE-FG09-87ER13811.

Supporting Information Available: Tables giving the total energies of the MH_2 and structures for the stationary points of $MH_2{\cdot}H_2$ in different arrangements and electronic configurations as well as the theoretical harmonic vibrational frequencies and IR intensities for the VH_4 and the low-spin $MH_2{\cdot}H_2$ (7 pages). This material is contained in many libraries on microfiche, immediately follows this article in the microfilm version of the journal, can be ordered from the ACS, and can be downloaded from the Internet; see any current masthead page for ordering information and Internet access instructions.

JA951376T